Visual Abstract

The influence of notch connection location on the short-term behaviour of timber-concrete composite beams, modelling of TCC beams and research for optimal locations, a numerical study

Hedmessaoud Zine Laabidine
Faculty of sciences and applied sciences, Department of Civil Engineering, Larbi Ben M'hidi University, Oum El Bouaghi, Algeria.
ali.zinelaabidine@gmail.com

Boudaoud Zeineddine, Ferhoune Noureddine
Laboratoire de développement durable et protection de l'environnement, Larbi Ben M'hidi University, Oum El Bouaghi, Algeria.
zboudaoud@yahoo.fr, ferhoune.noureddin@gmail.com

Abstract. Timber-concrete composite beams, known as TCC beams, have been widely used in rehabilitation or in new buildings where several types of connections are commonly inserted to ensure partial composite action between the timber joist and the concrete slab. The notched connections represent an effective system due to their strength and ductility and it is simple to cut from timber joists. As a result, a small number is needed for the composite beam to achieve high performance in terms of bending stiffness and load-carrying capacity.
This paper aims to develop a FE model for TCC beams with notched connections. It considers realistic interactions between different components. The developed FE model can satisfactorily predict the full range load-mid-span deflection curves and the failure mechanisms.
The predictions agree very well with the experimental results reported in the literature, including the stiffness and the load-carrying capacity.
After the validation, a numeric study was established, it aimed to research the optimal location of a notch connection between different proposed locations, to figure out which place must be installed to ensure high performance of the TCC beams.
As a result of this study, the notch installed at location P3000 was found to be the optimal location to assure the highest bending stiffness. While the maximum carrying capacity was achieved at location P3750.

Keywords. Timber-concrete composite, Notch connection, Notch Location, Optimal study, Optimal Location, Finite element analysis.

OPEN ACCESS

Citation: Zine Laabidine, H., Zeineddine, B., Noureddine, F., The influence of notch connection location on the short-term behaviour of timber-concrete composite beams, modelling of TCC beams and research for optimal locations, a numerical study, Frattura ed Integrità Strutturale, 64 (2023) 186-203.

Received: 20.12.2022
Accepted: 12.02.2023
Online first: 27.02.2023
Published: 01.04.2023

INTRODUCTION

Timber-concrete composite beams are composed of timber joists topped with a concrete slab, linked with a connection system to form a single composite structural element called "composite beam", to benefit from the qualities of each material, the compressive strength and the high stiffness of concrete, and the tensile strength of timber [1–4].
The use of shear connectors, having sufficient rigidity to limit sliding at the timber-concrete interface and to allow it to oppose the shearing forces generated by external forces, will help to develop a composite action [5]. The behaviour of TCC beams in large per cent depends on the performance of connections at the timber-concrete interface [6].
Consequently, the behaviour of a composite beam is limited between perfect behaviour which corresponds to beams with perfect adhesion between the timber joist and the concrete slab, and another without connection, where each one can slide freely when the composite beam is subjected to bending [7].
The geometric properties of this composite system will increase the strength of the beam, improve its bending stiffness and significantly reduce deflection under service loads [3], compared to a system without composite action, the behaviour of a composite system highly depends on the stiffness of its connection [8].
The notched connections are made of a cut in the beam and filled with concrete during the pouring of the slab [7,9]. The mode of failure of a notch alone is brittle [6,10], which corresponds to the mode of failure of concrete and timber in shear. For that reason, it is common practice to couple a transverse notch with a lag screw to ensure ductility and avoid separation and brittle failure [11].
Previous works have studied rectangular and triangular notch connections that are typically known for their high stiffness and strength [12]. A notch's design depends on the dimensions and load of a TCC beam. A notch can be reinforced with steel fasteners, screws or studs to increase shear capacity and minimise uplift [5]. Because of its high performance, precisely the high ductility[5] and strength and it is simple to cut from timber joist [13], so a small number is needed for the composite beam, the rectangular notch is considered an effective connection system to select for a TCC beam [12].
The factors that influence the performance of this type of connection are the geometry and dimensions of the notch, particularly its length, the geometry and property of the reinforcement, and its depth of penetration into the beam.
A longer notch will increase the stiffness and strength of the connection, while rebars or lag screws will provide plastic sliding and ductility [7].

STUDY OBJECTIVE

The common idea in the design of TCC beams is to concentrate the connections near the supports where the shear is higher. This prevents sliding between the timber joist and the concrete slab. Their spacing gradually increases up to the centre of the beam as the shearing force decreases [8]. The common practice of this idea is to place a notch connection at the most extreme point possible to ensure high bending stiffness and hence a high composite action of the TCC beam.
However, this idea does not take the strength of the connection into account. This exposes the notch at this extreme location to high shear forces, which can exceed the notch connection capacity and result in the loss of the composite action entirely.
The study of composite beams, with real dimensions based on laboratory tests, is often expensive and takes time, especially in large studies including multiple numbers of parameters, while resorting to finite element analysis gives an alternative tool to study these systems.
This work aims to establish a finite element model using ABAQUS software to predict the short-term bending-mid-span deflection behaviour of timber-concrete composite beams with notched connections.
After that, a numerical study was conducted using the validated model to investigate the effect of the notch location and search for a suitable location. This will provide maximal performance in terms of stiffness and strength for the TCC beam.

DESCRIPTION OF THE EXPERIMENTAL PROGRAM

A total of eleven TCC beams were designed for 8 and 10 m spans, constructed and tested to collapse under 4-point bending loads, as shown in Fig. 1.

All the beams are composed of a laminated veneer lumber (LVL) timber joist of 63 mm width and 400 mm high, topped with a concrete slab of 65 mm depth and 600 mm width, separated by an oriented OSB plywood interlayer as a lost framework [11,14].
The beams A1, B2, C1, E1, F1 and G1 are tested to collapse point while the beams B1, C2 and D1 were not tested for full destruction [11,14].
The beam G1 was a reference beam and the metal plate connections installed in the beam F1 require a full section. Therefore, these two beams are constructed with a double LVL joist and 1200 mm wide concrete flange, while the rest were constructed with reduced sectional geometry made of a single LVL joist of 63 mm width and 600 mm wide concrete flange as shown in Fig. 2 [11,14].

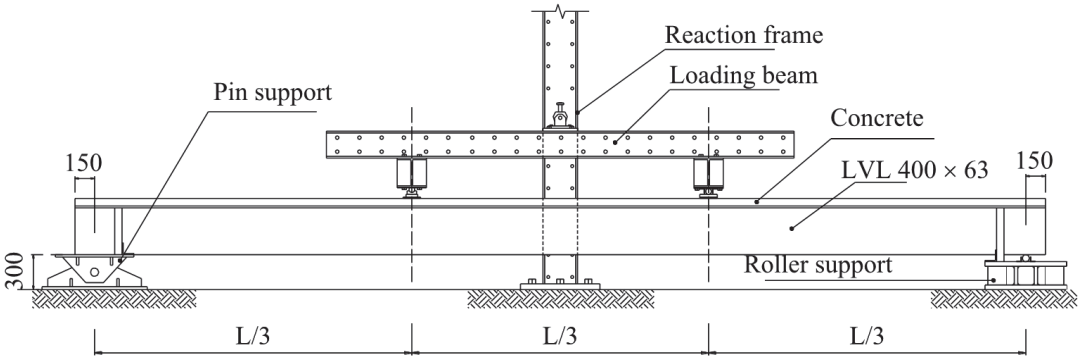

Figure 1: Four-point bending test of a TCC beam (dimensions in mm)[14].

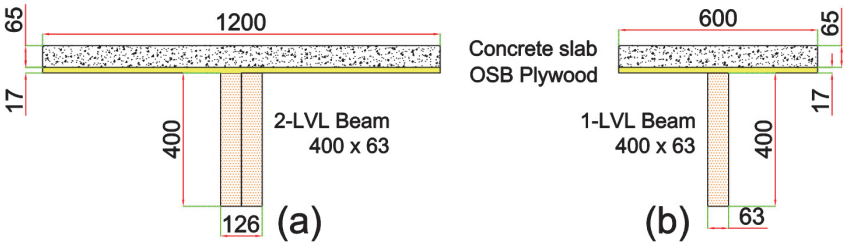

Figure 2: The cross-section of the tested TCC beams: (a) F1 and G1, (b) the reduced section of the rest (dimensions in mm) [14].

The connections type include notches cut in the timber and reinforced with a coach screw of 16 mm diameter (rectangular notches of 150 mm and 300 mm long) and triangular notch, and modified toothed metal plates pressed on the edge of the LVL joists, abbreviated R150, R300, T and P respectively, Fig. 3 presents these four connections.

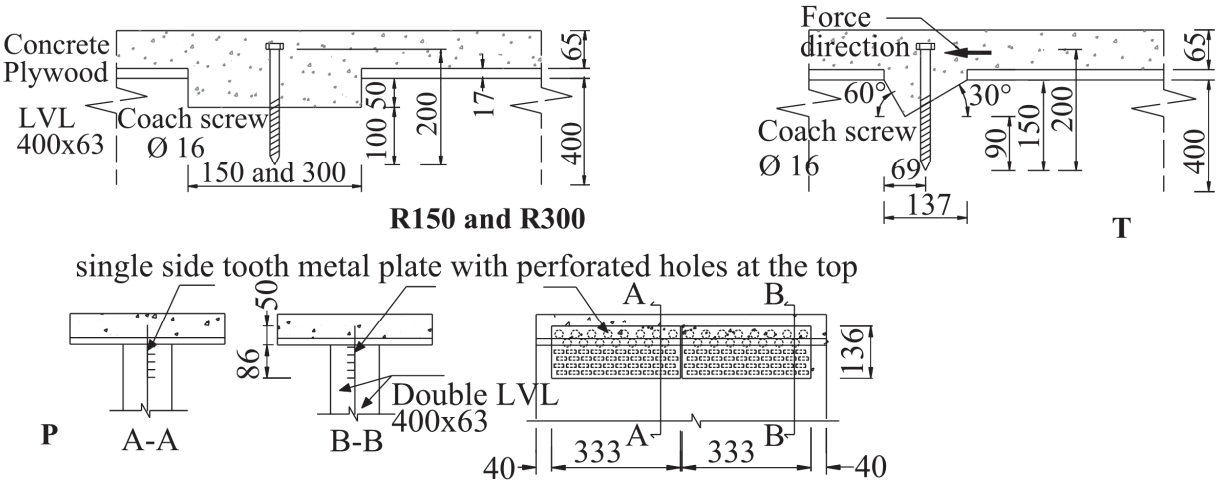

Figure 3: different connections: R150, T, R300 and P adopted in the experimental program by Yeoh [14].

The concrete compressive strength of the tested TCC beams are mentioned in Tab. 1:

N°	Beam	Concrete compressive strength at test f'c (MPa)
1	A1,B1,C2	58
2	C1, D1,F1	54.4
3	G1	48.2
4	B2	38.8

Table 1: Concrete compressive strength of the tested TCC beams[14].

The design of the tested TCC beams including the geometry, the type and the configuration of the connections are illustrated in Fig. 4:

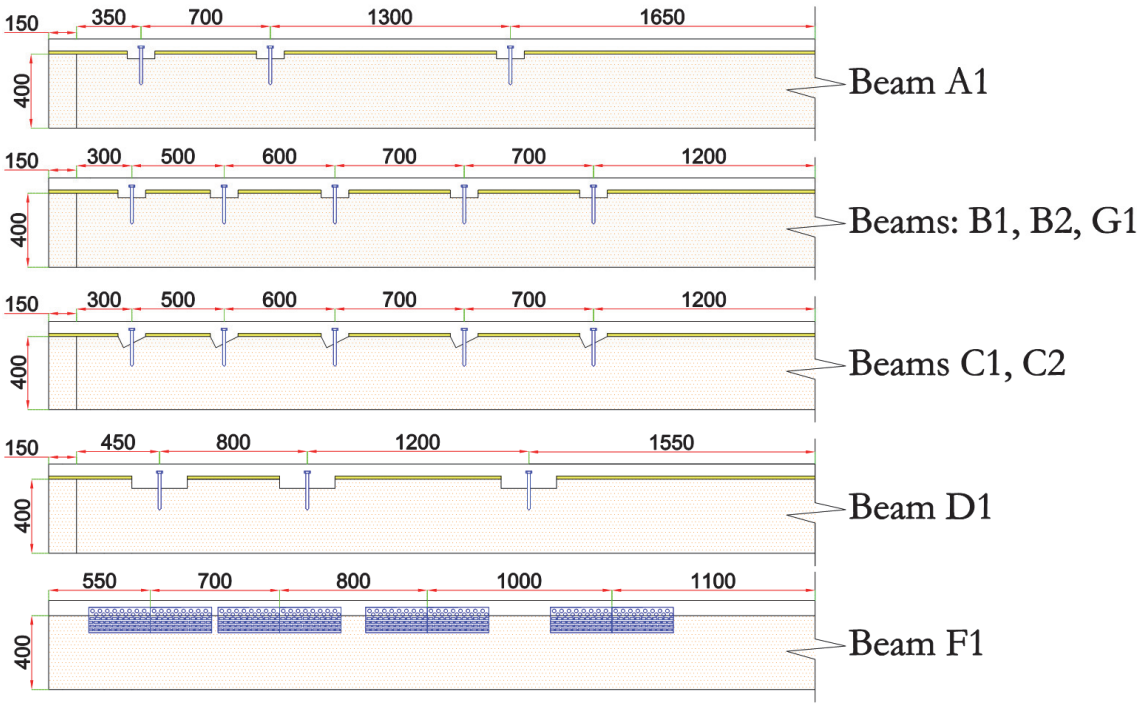

Figure 4: The design of the tested TCC beams (dimensions in mm) [14].

FINITE ELEMENT MODEL ESTABLISHMENT

Geometry

A three-dimensional (3D) model was built in ABAQUS for the eight TCC beams shown in Fig. 4, this software was selected for this research work because of its high performance and precision. It is capable of modelling non-metal materials as well as reinforced concrete with a nonlinear response. Furthermore, it is capable of predicting and displaying cracking and crushing patterns [15].

The geometry, material characteristics, loading, and boundary conditions of the FE models are similar to those of the tested beams previously described in the experimental part (Fig.4).

Due to the symmetry of geometry, loading and boundary conditions, only one-half of the TCC beams were modelled with an (OX) symmetry plan considered at the mid-span of the composite beam, except for beam F1 which is modelled with two plans of symmetry.

The numerical models of the TCC beam consist of five components, which are: one-half of the concrete slab, one-half of the LVL timber beam, one-half of the OSB plywood, the reinforcement rebars, and one rolling support.

The LVL joist and the concrete slab are simulated as independent solid 3D objects because of the complicated geometry and the cuts into the timber beams. The installed plywood OSB interlayer as a separation between the concrete slab and the LVL joist as a lost framework is also simulated as a solid 3D object of 17 mm depth.

Both the reinforcements and the screw connectors are embedded in the concrete slab, so the "embedded region" option was chosen.
All parts of the TCC beam models were assembled in their proper locations.
All the contacts between the components are defined as "Normal contacts", which is defined by the "hard contact" option, while "penalty" was selected for tangential behaviour with different friction coefficients.
A loading displacement was imposed at a reference point coupled to the load application surface at the third span of the TCC beam. While the loading force is obtained by measuring the reaction force at the same point. This procedure enables the model to capture the maximum force registered in the bending process. The mid-span deflection was extracted from a reference point set at mid-span as shown in Fig. 5.

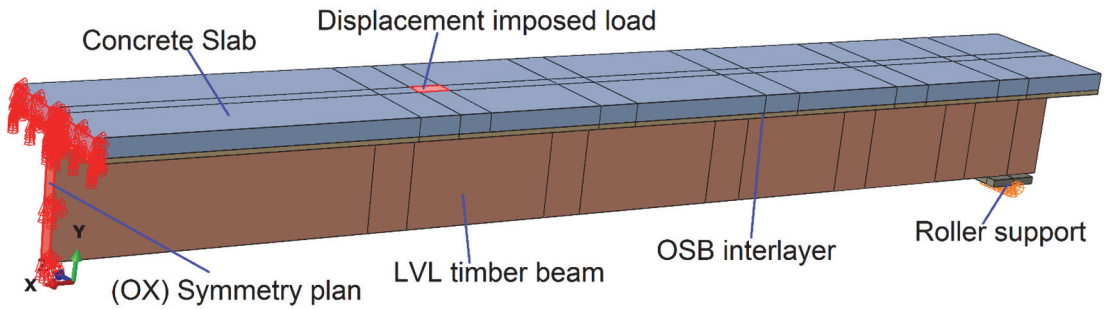

Figure 5: The modelled TCC beam with different components and boundary conditions.

Mesh

The concrete slab, the LVL beam, the OSB plate and the screw connectors were modelled using the 8-node linear brick element with reduced integration "C3D8R". The element has the potential to be used in a wide range of nonlinear analyses including plasticity, contact, large displacements, and failure [16].
The concrete reinforcement was modelled using the truss element T3D2, which is a linear element with two nodes.
In order to reduce computational effort, a finer mesh was applied to the notch connection and the surrounding LVL region. For the rest of the model, a reasonable mesh was used.
The general view of finite element mesh of the simulated TCC beams is presented in Figs. 6-7. A precise view of the connectors where a finer mesh is applied is shown in Fig. 8.

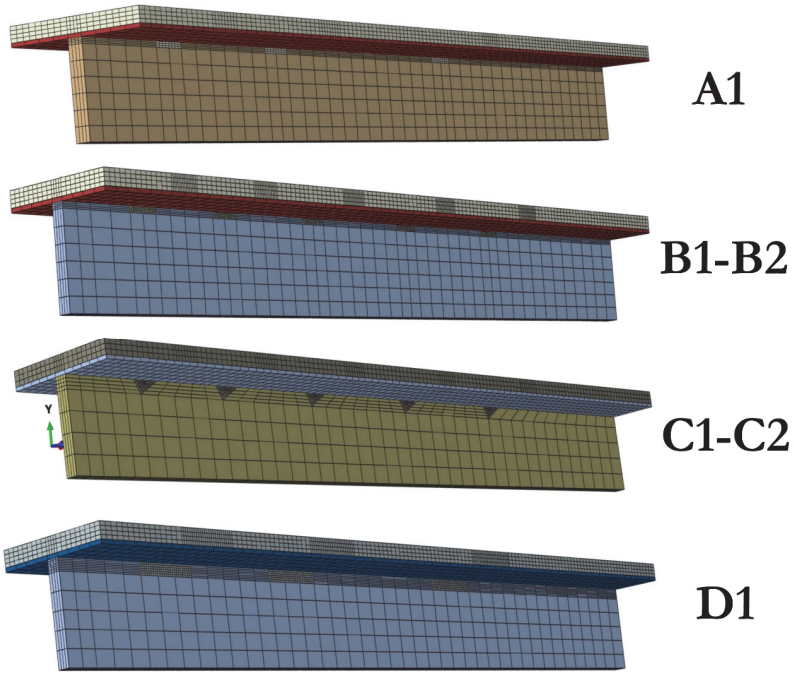

Figure 6: mesh of the simulated TCC beams with reduction section: A1, B1, B2, C1 and C2.

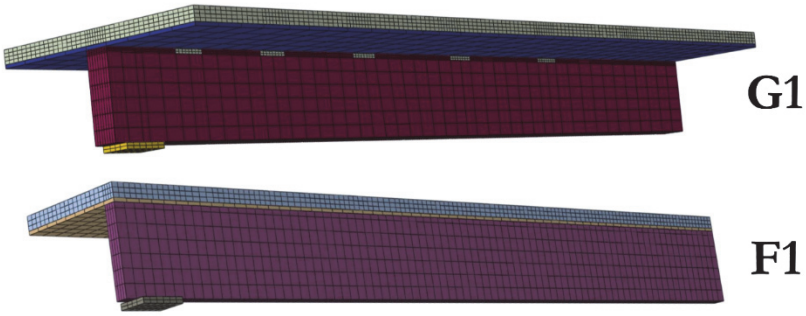

Figure 7: mesh of the simulated TCC beams with full section: G1 and F1.

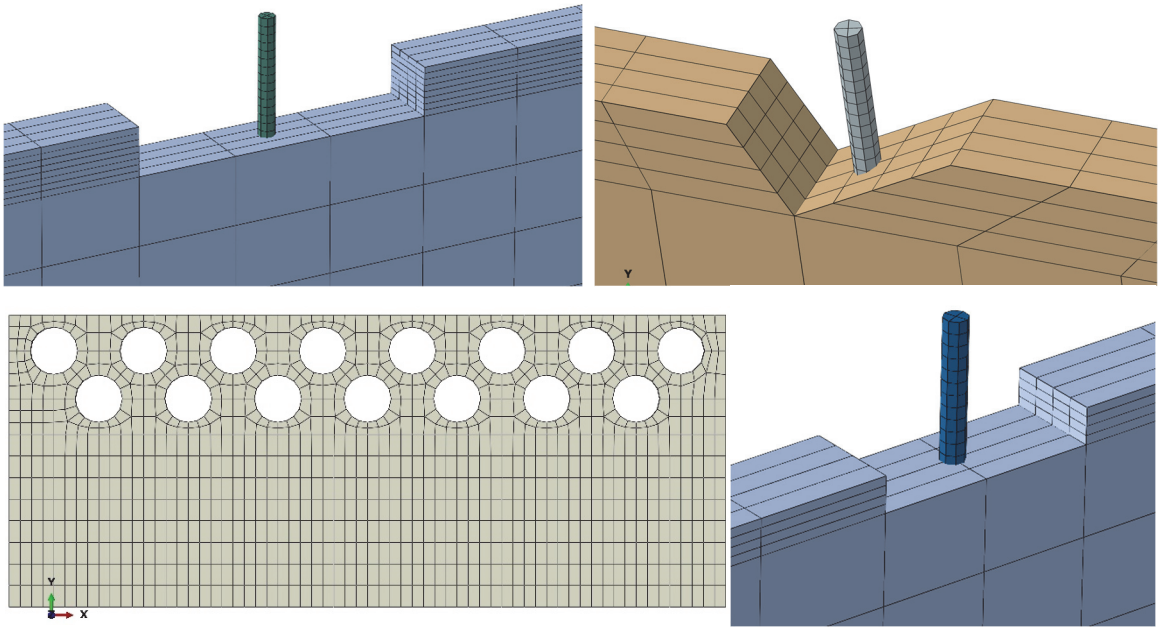

Figure 8: Modelling of R300 rectangular notch, R150 rectangular notch and triangular notch with embedded screw of 16 mm diameter and toothed metal plate connection.

Materials constitutive models

The LVL Timber is simulated as an orthotropic material, the constitutive relationship for three-dimensional orthotropic linear elasticity is given by Eqn. 1:

$$\begin{Bmatrix} \varepsilon_{11} \\ \varepsilon_{22} \\ \varepsilon_{33} \\ 2\varepsilon_{12} \\ 2\varepsilon_{13} \\ 2\varepsilon_{12} \end{Bmatrix} = \begin{vmatrix} \frac{1}{E_{11}} & \frac{-\nu_{21}}{E_{22}} & \frac{-\nu_{31}}{E_{22}} & 0 & 0 & 0 \\ \frac{-\nu_{12}}{E_{22}} & \frac{1}{E_{22}} & \frac{-\nu_{32}}{E_{22}} & 0 & 0 & 0 \\ \frac{-\nu_{21}}{E_{11}} & \frac{-\nu_{23}}{E_{22}} & \frac{1}{E_{33}} & 0 & 0 & 0 \\ 0 & 0 & 0 & \frac{1}{G_{23}} & 0 & 0 \\ 0 & 0 & 0 & 0 & \frac{1}{G_{13}} & 0 \\ 0 & 0 & 0 & 0 & 0 & \frac{1}{G_{12}} \end{vmatrix} \bullet \begin{Bmatrix} \sigma_{11} \\ \sigma_{22} \\ \sigma_{33} \\ \tau_{12} \\ \tau_{13} \\ \tau_{12} \end{Bmatrix} \quad (1)$$

while:

E_{ii} is modulus of elasticity in i direction.
ν_{ij} is poison's ratio of orthotropic material.
G_{ij} is shear modulus in plane with normal of i and in the j direction.
σ_{ij} is normal Stress in i direction.
τ_{ij} is shear stress in plane with normal of i and in the direction of j.
ε_{ij} is strain vector.

For this numerical study, a realistic parameters of the orthotropic behaviour of the timber LVL are adopted and mentioned in Tab .2 [17]:

E_{11}	E_{22}	E_{33}	ν_{12}	ν_{13}	ν_{23}	G_{12}	G_{13}	G_{23}
12000	485	280	0.0464	0.365	0.309	600	600	24

Table 2: Timber LVL elastic orthotropic parameters [17].

The tensile strength is 33.4 MPa, and the shear strength is 5.3 MPa [18]. For the plastic behaviour, the option "potential" was added with the following parameters:

$$R_{11}=\frac{\sigma_0}{\sigma_{eq}} \tag{2}$$

$$R_{22}=R_{33}=\frac{\sigma_{90}}{\sigma_{eq}} \tag{3}$$

$$R_{12}=R_{13}=R_{23}=\frac{\sqrt{3}\sigma_v}{\sigma_{eq}} \tag{4}$$

while

σ_0 is the yielding strength in the direction parallel to the grain.
σ_{90} is the yielding stress in the direction perpendicular to the grain.
σ_{eq} is the equivalent yielding strength for isotropic behaviour, and σ_{eq} is taken as 33.4 MPa in the present paper and it is the reference yield. In this case, it equals σ_0 [9].

The OSB plate is simulated as an isotropic material with an elastic modulus equal to 3253 MPa [19].
The concrete grade adopted is the same in the experimental program with an average density (ρ) of 3405 Kg/m^3.
The calculated elastic modulus depends on the concrete compressive strength (f'c) and it is given by Eqn. 5 [11]

$$E_c=(3320\sqrt{f'_c}+6900)*\left(\frac{\varrho}{2300}\right) \tag{5}$$

Its values for each TCC beam is listed in Tab. 3.

N°	Beam	f'c(MPa)	Ec (MPa)
1	A1,B1,C2	58	34413.26
2	C1, D1,F1	54.4	33560.79
3	G1	48.2	32023.63
4	B2	38.8	29490.20

Table 3: The calculated concrete elastic modulus for each TCC beam.

The concrete damaged plasticity (CDP) available in ABAQUS material library was employed [20]. The material dilation angle (Ψ), the eccentricity (ε), the ratio of biaxial compressive strength to uniaxial compressive strength (f_{b0}/f_{c0}) and tensile to compressive meridian ratio (K) are mentioned in tab. 4.

Dilation angle	Eccentricity	f_{b0}/f_{c0}	K	Viscosity parameter
35	0.1	1.16	0.667	0.01

Table 4: Concrete damage plasticity (CDP) parameters adopted in the simulation.

An example of the compressive and tensile behaviour for a concrete grade 38 MPa is shown in Fig. 9:

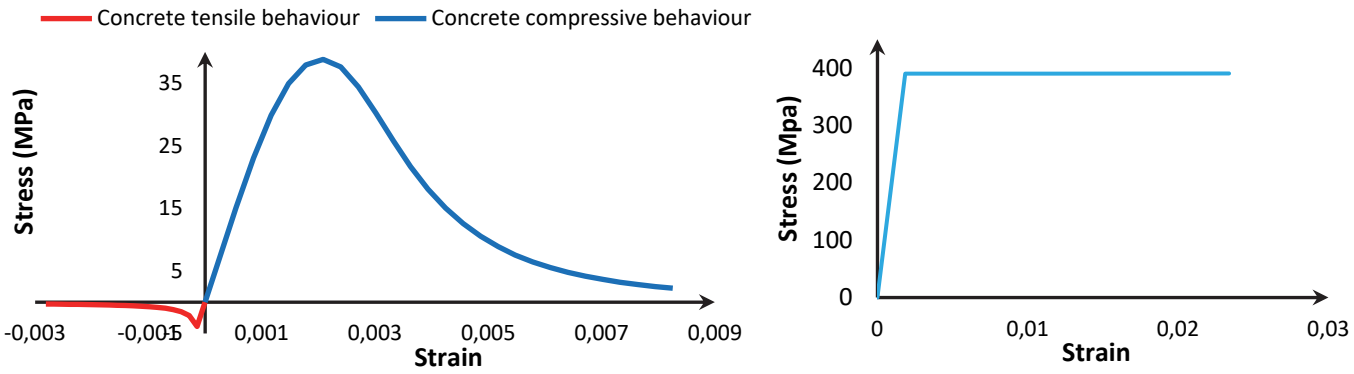

Figure 9: Example of the behaviour curves of concrete grade 38 MPa and Steel stress-strain curve.

In order to model the steel, a bilinear elastoplastic behaviour law was used. The stress-strain curve of steel adopted in the simulation is given in Fig. 9 (right) with a young modulus of 210,000 MPa, a Poisson ratio υ=0.3 and a yield limit stress of 400 MPa.

Validation of the FE models

The load-mid-span deflection curves of the TCC beams, obtained by the numerical analysis are displayed and validated and by tests [14] in Figs. 10-12. The full composite and no composite limits are also added.

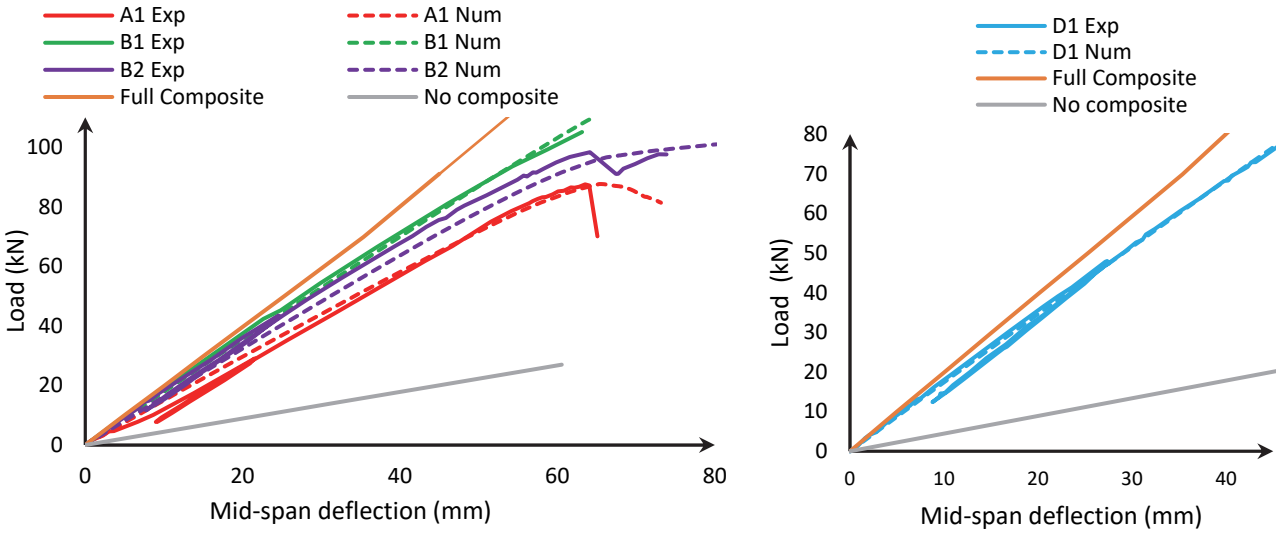

Figure 10: The load-mid-span deflection curves of the modelled TCC beams with rectangular notch connections R150 (left) and R300 (right) compared with the experimental results.

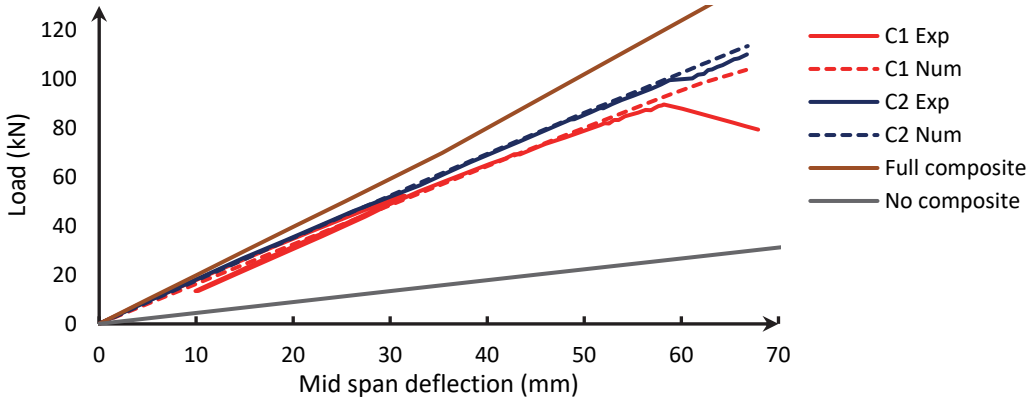

Figure 11: The load-mid-span deflection curves of the TCC beams C1 and C2 with Triangular notch connections compared with the experimental curves.

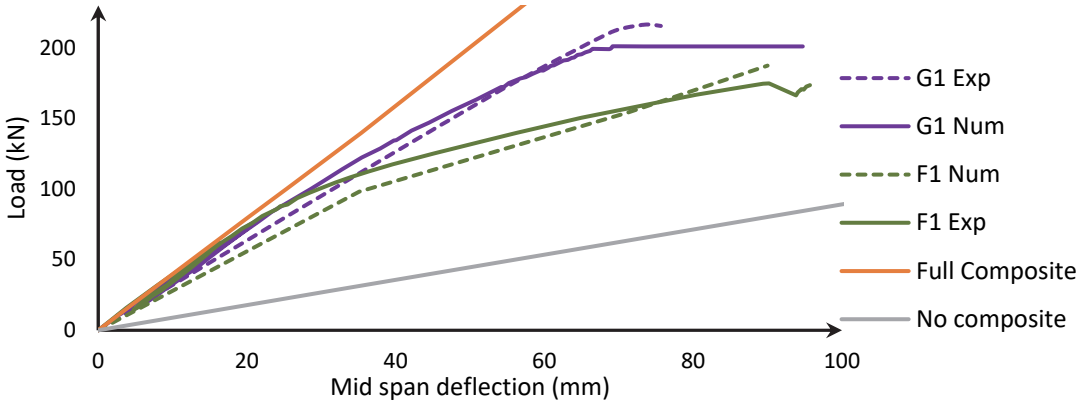

Figure 12: The load-mid-span deflection curves of the TCC beams F1 and G1 compared with the experimental curves.

A general comparison of the bending stiffness K_{TCC} and the maximum load are reported in Tab. 5:

N°	Beam	F_{max} (kN)		Error (%)	K_{TCC} (N/mm)			Error (%)	
		EXP	FEM	FEM/EXP	EXP	FEM	Anal	FEM	Anal
1	A1	87.3	87.64	0.39	1363.25	1336.30	1498.92	-3%	15%
2	B1	105	109.37	4.16	1664.48	1705.59	1642.05	3%	-2%
3	B2	97.5	103.76	6.42	1520.54	1449.89	1609.72	-7%	8%
4	C1	89.7	120.54	34.38	1541.39	1592.81	1791.40	5%	23%
5	C2	110	113.42	3.11	1647.80	1696.77	1797.61	4%	13%
6	D1	80.8	81.82	1.26	1745.52	1701.12	1787.36	-3%	3%
7	F1	174	187.4	7.70	1929.34	2082.22	3492.13	15%	154%
8	G1	201	216.51	7.72	2875.43	3043.10	3254.37	9%	19%

Table 5: Validation of the main results: strength and stiffness obtained by numerical analysis and the experimental [17].

The first observation is that the FEM curves are on the safe side compared to the experimental curves.

More particularly the results of the simulated beams exhibited high accuracy in terms of stiffness, this can be observed in Figs. 10-12, where all the load-deflection curves are in proximity to the test curves. The maximal force obtained for the simulated beams with reduced section was very close to that obtained in tests with no significant differences in strength in the case of the beams: A1, B1, B2, C2, and D1.For the beams F1 and G1 with full section and the beams C1 and D1, a slight difference can be detectable, where the difference up to its maximal value of 34% in the case of the beam C1. Nevertheless the FEM exhibited accurate outcomes for the majority of the simulated beams where it stays better than the obtained by the analytical method.
In terms of failure detection the two types of failure mechanisms can be displayed by the model with satisfactory precision. The first type is the fracture by the tension of the LVL joist under the loading points at one-third of the span with no apparent sign of failure in connections for well-designed beams as shown in Fig. 13.

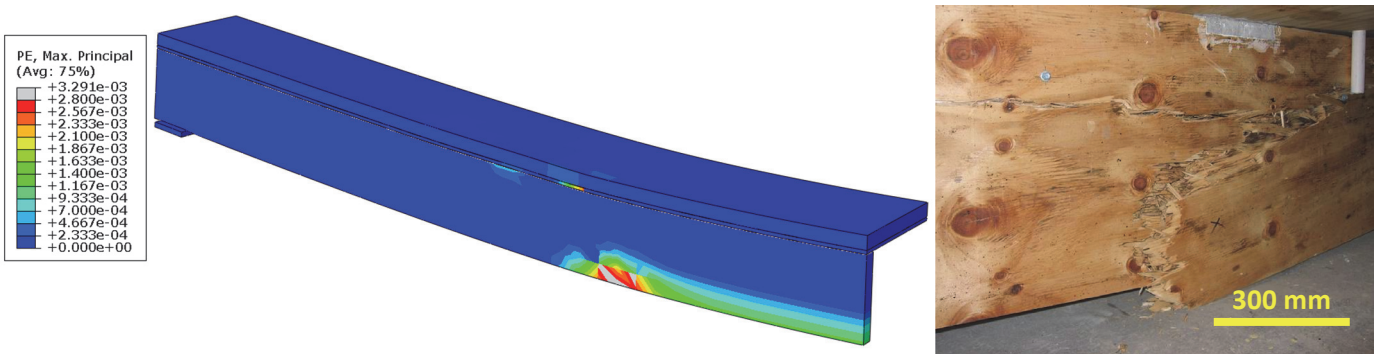

Figure 13: Plastic strain distribution displayed in the simulation compared to LVL bending tension failure obtained at one-third span of the beam G1 [11].

The second type is shear failure of the connection in the under-designed beams where less number of connection are installed.
The appearance of plastic strain in the model is an indication of cracks. The plastic strain propagates along the notch as a sign of crack growth until it completely separates from the slab, causing the fracture of the connection and the deterioration of the concrete surrounding the coach screw.

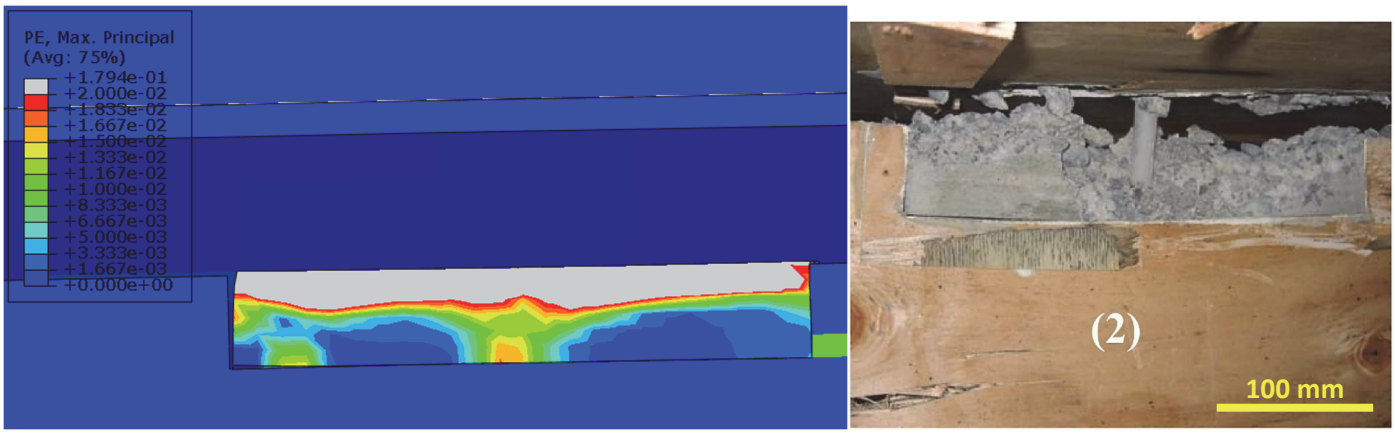

Figure 14: Plastic strain distribution displayed at the notch connection compared to failure mode obtained in the test.

This failure mode of the notch connection was similar to what was observed in the push-out tests, where it was found that the concrete strength had a significant influence on the shear strength of the connection, and thus, the load-bearing capacity of the composite beam [14].
In conclusion, the model can satisfactorily predict the short-term behaviour of the timber-concrete composite beams with notched connections specifically predict the stiffness and the maximum load carrying capacity either in the well-designed beams or in the under-designed beams with different dispositions and variety of connections which implied the validation of the model.

RESEARCH FOR THE OPTIMAL LOCATION

Objective

The study aims to investigate the short-term behaviour of timber-concrete composite beams employing previously approved FEM. Its specific goal is to investigate the load-mid-span deflection behaviour of the TCC beam characterised by the maximum registered load and the TCC beam stiffness. These are the two main qualities requested in the TCC beam, which are strongly affected by the notch location and the notch length. This study aims to improve the performance of the TCC beam by maximising its strength and stiffness. This leads us to an optimal study of the TCC beam affected by the notch location. In other words, find the most suitable location for a notch connection to maximize the stiffness and strength.

Method

To find the optimal location, only one notch was installed at once in the composite beam at a specific location.
Six locations are selected namely: P2500, P3000, P3250, P3500, P3750 and P4000, which represent the distance from the mid-span of the beam to the notch centre. Another location P2000 was added later to visualise the variation in stiffness around the location P3000. Four rectangular notches were selected. They all have the same depth of 25 mm and the same width of 63 mm. Each notch connection has a different length of 50, 100, 150, and 200 mm.
This variation in length is necessary to verify that the optimal location is not affected by its length. The notch length is the chosen parameter because of its high effect on the performance of the notch connection and consequently on the TCC beam behaviour. The notch is equipped with a lag screw of 16 mm diameter.
With only one notch connection installed every time at six different locations, twenty-four (24) load-mid-span curves are plotted to represent twenty-four (24) separate cases. These curves are grouped by location. The studied TCC beam is illustrated in Fig. 13.

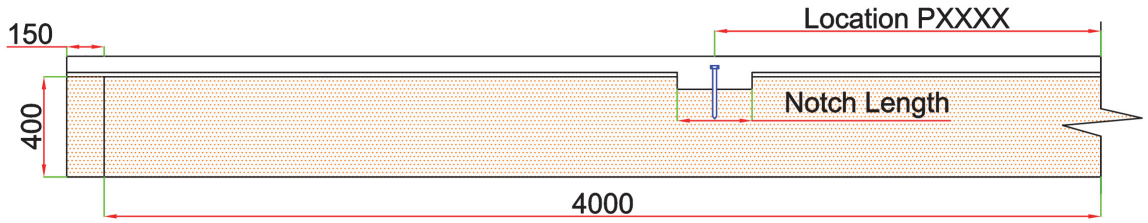

Figure 15: The parameters of this optimal study.

The following abbreviations listed in Tab.6 was considered to make easy the interpretation of the results:

Abbreviation	designation
R 50	Rectangular notch of 50 mm length, 63 mm width and 25 mm depth.
R 100	Rectangular notch of 100 mm length, 63 mm width and 25 mm depth.
R 150	Rectangular notch of 150 mm length, 63 mm width and 25 mm depth.
R 200	Rectangular notch of 200 mm length, 63 mm width and 25 mm depth.
P 2500	The notch is located 2.5 m from mid-span.
P 3000	The notch is located 3 m from mid-span.
P 3250	The notch is located 3.25 m from mid-span.
P 3500	The notch is located 3.5 m from mid-span.
P 3750	The notch is located 3.75 m from mid-span.
P 4000	The notch is located 4 m from mid-span.

Table 6: the abbreviations adopted in the study.

RESULTS AND DISCUSSIONS

Fig. 16 illustrates the load-mid-span deflection curves of the twenty four cases.

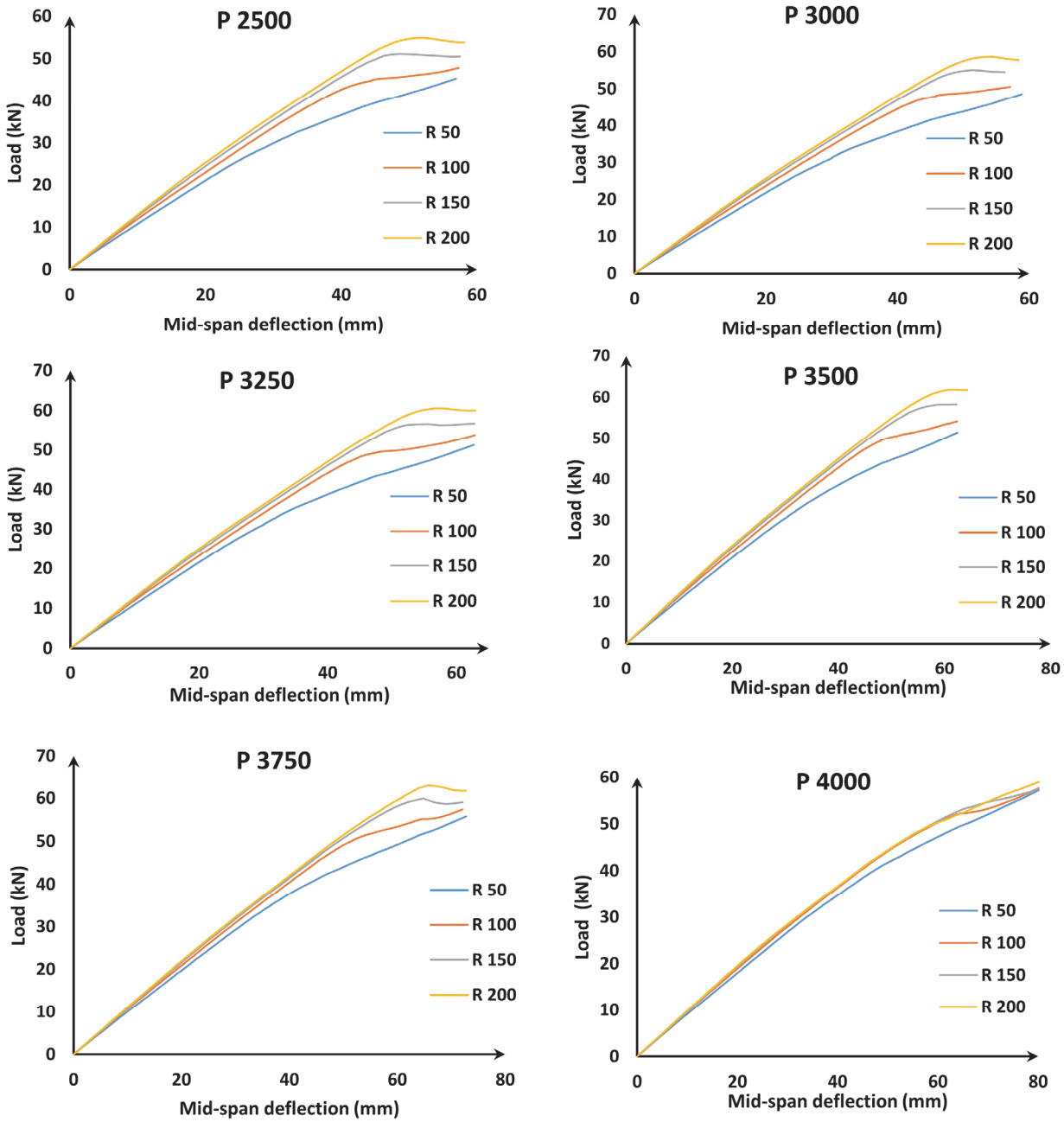

Figure 16: Load-mid-span curves of all bending cases of R50, R100, R150 and R200 in different locations.

Modes of failure

Generally, with only one connection installed on each beam, all the beams are under-designed, and they appear to behave similarly because the insufficient number of connections leads to losing the composite action before any failure in the principal parts consequently the timber beam and concrete slab stay intact.

The visualisation of the twenty-four bending beams according to their failure can be reduced to three main categories A, B and C illustrated in Fig. 17. Which are:

A) Shear failure of the notch without remarkable effect on the composite action of the TCC beam.

B) Shear failure of the LVL.
C) Shear failure of the notch can clearly show a loss in composite action.

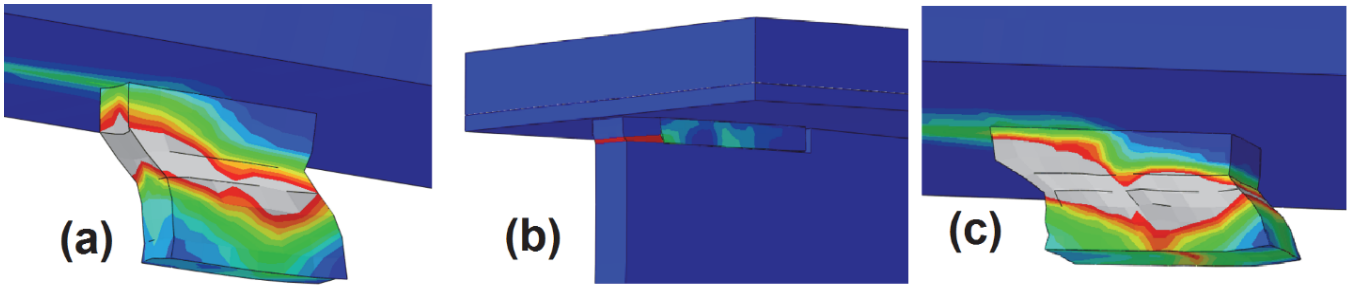

Figure 17: Plastic strain distribution show shear failure of the connection: (a) R 50 at position 2m, (b) in timber for R200 located at 04 m and(c) shear failure of R100 Located at 3 m.

In this numerical analysis, the shear failure is displayed by the visualisation of the plastic strain distribution. These three different mode of failure at the timber-concrete interface are explained as follow:

A) Shear failure of the notch without remarkable effect on the composite action of the TCC beam. (Fig. 17 (a))
The load-mid-span deflection curves of the TCC beams equipped with the connection notch of 50 mm length (R50) in all locations do not show a clear limit in strength or a remarkable loss in the composite action. The R50 has a small length, so a small capacity to resist the shear effort. As a result, this notch with such small dimensions does not have a considerable effect on the composite action.
The small length of the R50 makes the TCC beam perform less compared to the others equipped with connections of big dimensions. The strength and stiffness stay less than the others.

B) Longitudinal shear failure of the timber LVL (Fig. 17 (b))
This type of failure is observed in the case of the notch connection R 200 located near the bearing support specifically at the location P4000. The R 200 connection with such big length has sufficient strength to cause this type of damage to the small part left of the LVL that can not resist the resulting shear forces. So a longitudinal shear failure in the LVL joist was observed in this case.
It is important to notice that the location P4000 presents an exception because all the connections with different lengths located in this location do not show any difference in terms of stiffness or strength.

C) Shear failure of the connection which agrees with loss in composite action shown in load-mid-span curves (Fig. 17 (c))
The earliest sign of failure of under-designed beams is the appearance of plastic strain in the connection, which occurs due to the low resistance of concrete when shear loads are applied to it.
Plastic strain propagates along the connection as a mark of crack growth until it separates completely from the slab, causing the connection to fracture. The two principal components, the timber joist and the concrete slab can slide freely on each other. They are only connected by the lag screw, and because of the deterioration of the surrounding concrete, the screw alone is subjected to shear/bending effort and will be plasticized.
The timber joists slide freely under the concrete slab without resistance from the connection system.
The mid-span deflection increases without any variation in the bending load.
In terms of stiffness, the TCC beam lost its composite action.
After that, the LVL beams are the only structural element resisting the bending load.

Extraction of bending stiffness and strength

Fig.18 illustrates the typical curve for an under-designed TCC beam, the extracted initial stiffness K_i, the extracted service stiffness K_{ser}, and the maximal bending force F_{max}.

From the load-mid-span deflection curves (Fig. 16), the initial bending stiffness K_i, the final service bending stiffness K_{ser}, and the TCC beam strength F_{max} are extracted. The initial bending stiffness Ki is the stiffness calculated at the first response of the TCC beam. The final service bending stiffness K_{ser} is the stiffness that corresponds to the allowed service mid-span deflection equal to L/300 [21]. The TCC beam strength F_{max} is the maximal bending force attended during the execution of the simulation. At this point, the resulting shear force has reached the capacity of the notch.

The initial bending stiffness, the service bending stiffness, the TCC strength of all beams were extracted from the bending curves and summarised in Tab. 7. A general comparison is made in Figs. 19-21.

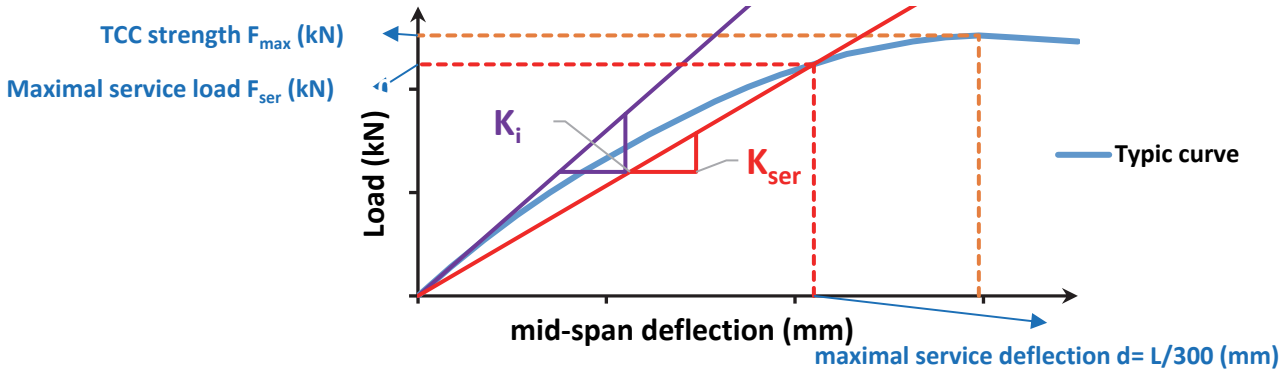

Figure 18: Typical load–mid-span deflection curve of the under-designed TCC beam.

Connection	Location (mm)	K_i(N/m)	K_{ser} (N/m)	F_{max} (kN)	Loss in stiffness	Failure category
	2000	1007	942		6%	A
	2500	1147	1024	38.1	11%	A
	3000	1172	1062	42.3	9%	A
R50	3250	1143	1057	43.2	8%	A
	3500	1090	1029	44.8	6%	A
	3750	1021	981	49.5	4%	A
	4000	917	896	47.5	2%	A
	2000	1098	1023		7%	C
	2500	1210	1133	45.3	6%	C
	3000	1252	1167	48.5	7%	C
R100	3250	1214	1143	49.8	6%	C
	3500	1152	1099	50.5	5%	C
	3750	1066	1035	55.2	3%	C
	4000	954	937	52.3	2%	C
	2000	1138	1065		6%	C
	2500	1278	1196	51.1	6%	C
	3000	1288	1220	55.1	5%	C
R150	3250	1245	1193	56.6	4%	C
	3500	1177	1144	58.6	3%	C
	3750	1085	1067	60.0	2%	C
	4000	966	957	54.9	1%	C
	2000	1165	1099		6%	C
	2500	1308	1232	54.8	6%	C
	3000	1314	1249	58.6	5%	C
R200	3250	1267	1219	60.6	4%	C
	3500	1193	1165	61.8	2%	C
	3750	1098	1082	63.0	1%	C
	4000	975	960	50.3	2%	B

Table 7: The extracted values of initial bending stiffness, elastic strength and ultimate strength.

Initial bending stiffness and service bending stiffness

The TCC beams achieve the maximal initial bending stiffness K_i and the maximal service stiffness K_{ser} in all locations with the notch connection R200. Because of the long length, the TCC beams have high stiffness and strength.

In all cases, the TCC beams with long notches in the same location always exhibit a higher initial bending stiffness Ki and also a higher service bending stiffness K_{ser} compared to the beams with short notches. Therefore, the TCC beam with a long notch performs better in terms of stiffness.

The TCC beams equipped with notch connections with different lengths at location P3000 offer the best performance in terms of stiffness compared to other locations Fig 19-20. The initial Stiffness Ki and the service Stiffness K_{ser} reached their maximal values at this location. As a result, it proved that the location P3000 is the most suitable location as shown in Figs. 19-20.

For the case of the notches at this location (P3000), Doubling the notch length from 50 mm to 100 mm improves the initial bending stiffness Ki up to 7% (from 1172 to 1252 N/m), up to 10% (from 1172 to 1288 N/m) for the case of 150 mm and finally up to 12% (from 1172 to 1314 N/m).

For the case of the notches in location P3000, Doubling the notch length from 50 mm to 100 mm improves the final elastic stiffness K_{ser} up to 12% (from 908.1 to 1019.8 N/m), up to 18% (from 908.1 to 1072.2 N/m) for the case of 150 mm and finally up to 19% (from 908.1 to 1077.5 N/m).

Total improvement in initial stiffness

The total improvement of initial stiffness K_i by increasing the notch length from 50 mm to 200 mm is registered at the location P2500 (from 1147 to 1308 N/m). This represents a difference of 160 N/m, which represents an improvement of 14% in the initial stiffness. The location P2500 is determined as the most sensitive location. It has the maximal effect on the stiffness by increasing the length of the notch at this location.

The maximal improvement of initial stiffness K_i by changing the notch location is remarked in the case of the notch R200 from P4000 to the location P3000 (from 975 to 1313.6 N/m). This represents a difference of 339 N/m which represents an improvement of 35% in initial stiffness. This confirms that the location of the connection has a crucial effect on the performance of the TCC beams.

Total improvement in final service stiffness

The total improvement of service stiffness K_{ser} by increasing the notch length from 50 mm to 200 mm is registered at the location P2500 (from 1024 to 1232 N/m). This represents a difference of 208 N/m, which represents 20%.

The maximal improvement of service stiffness K_{ser} is achieved at the notch R200 by changing the notch location from P4000 to P3000 (from 975 to 1313.6 N/m). This represents a difference of 339 N/m, which represents 35%.

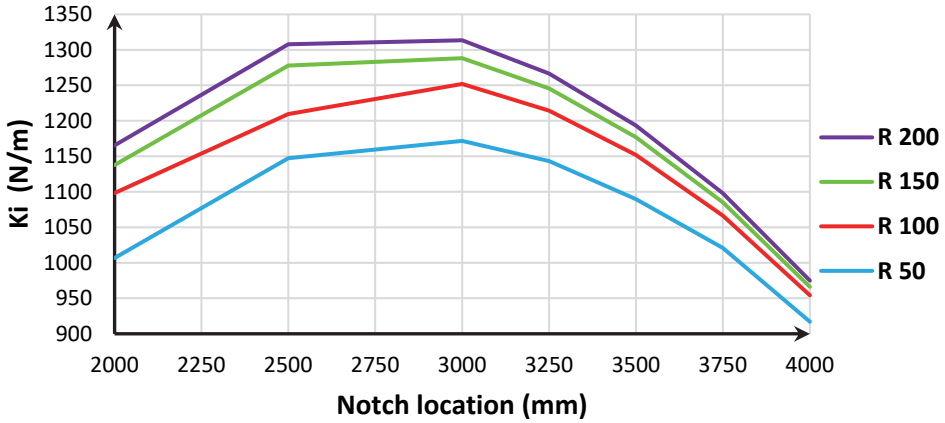

Figure 19: the effect of notch length and its location on the initial bending stiffness.

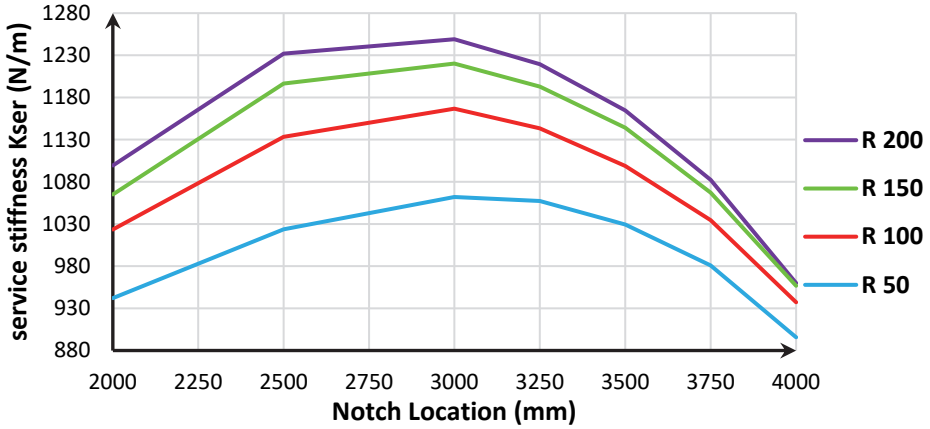

Figure 20: The effect of notch length and its location on the service bending stiffness.

TCC beams strength

The TCC beam strength is achieved in all locations by the notch connection R200. The long length provides the TCC beam with the highest strength.

The TCC beams with long notches in every case, regardless of the location, demonstrate a higher strength compared to the beams with short notches except for P4000, where the length of the notch near the bearings represents an unfavourable parameter, causing the weakening of the portion of the LVL that is set aside to be resistant to the shear forces generated at the interface between the two principal components, the LVL joist and the concrete slab. Despite that, this suggests that the longer the notch at the right location, the higher the strength of TCC beams.

The TCC beams equipped with notch connections of different lengths reached their maximum strength at location P3750. The strength curves point to an optimum at this location.

For the case of the notches in this location P3750, Doubling the notch length from 50 mm to 100 mm improves the maximal strength F_{max} by 13% (from 49 to 55.2 kN), up to 22% (from 49 to 60 kN) for the case of 150 mm notch length and finally up to 29% (from 49 to 63 kN) for the case of 200 mm notch length.

Improvement in strength

The total improvement of strength F_{max} by increasing the notch length from 50 mm to 200 mm is registered at the location P2500 (from 38.1 to 54.8 kN), a difference of 16.7 kN, which represents an improvement of 43% in strength. The location P2500 is determined as the most sensitive location. Just increasing the length of the notch at this location will enhance the strength of the TCC beam.

The maximal improvement of strength F_{max} by changing the notch location is observed with R50 from P2500 to location P3750 (from 38.1 to 49.5 kN), a difference of 11.4 kN, which represents an improvement in the strength of 30%. This confirms that the TCC beam strength can be improved by 30% just by moving the connection 1.25 m along the beam.

Fig. 21 presents the effect of the notch location on the load carrying capacity.

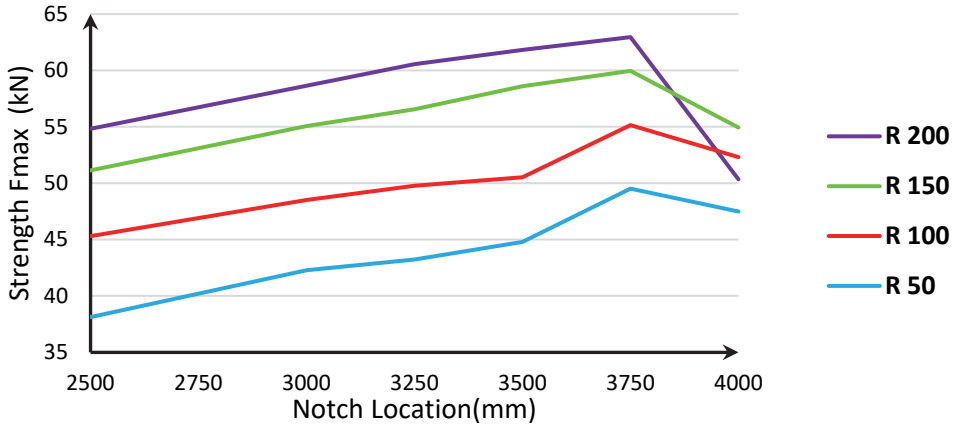

Figure 21: The effect of notch length and its location on the TCC beam strength.

Conclusion

This paper investigates the short-term behaviour of timber-concrete composite beams with various notch lengths situated in different locations along the composite beam using the finite element method based on developing a simple model supported by ABAQUS software. After validating the preliminary results which the model exhibited a satisfactory precision compared to the experimental outcomes, a numeric study was established.

The optimal study aimed to determine the effect of the notch location and the notch length on the short-term behaviour of the timber-concrete composite beams, specifically on the TCC beam bending stiffness and the TCC strength.

The conclusions of this study are listed into two main categories: the effect of the notch connection location and the effect of the notch length.

Effect of the location

- This study found that the notch connection location has a significant effect on the short-term behaviour of the TCC beam.

- TCC beams perform better with a small notch at the proper location rather than a large notch poorly situated. Precisely, the TCC beam exhibits higher stiffness and higher load-carrying capacity.
- In terms of stiffness, the location P3000 was found to be the optimal location for the TCC beam to ensure high bending stiffness. Moving the notch to this optimal location can increase the stiffness up to 35%.
- P3750 is the most suitable location for installing a notch connection to achieve higher strength. Moving the notch to this optimal location can increase the bending strength by 30%.
- The length of the notch has no effect on these locations. Therefore,
- In the end, this study confirms that the location of the notch must be well-considered in any design.
- The notch length does not affect these locations. In another words these optimal location were found to be stable.
-

Effect of the notch length

- This study found that the notch length has a significant effect on the short-term behaviour of the TCC beams.
- In all cases, the increase in the notch length increases the initial bending stiffness of the TCC beams. The long notch gives the TCC beam the highest bending stiffness and strength except for an extreme location near the supports.
- The increase in the notch length from 50 mm to 200 mm can improve the bending stiffness by 20% and the load carrying capacity by 43%.

REFERENCES

[1] Yeoh, D., Fragiacomo, M. (2012). The Design of a Semi-Prefabricated LVL-Concrete Composite Floor, DOI: 10.1155/2012/626592.

[2] Cimadevila, J.E., Chans, D.O., Gutiérrez, E.M., Riestra, F.S. (2020). Testing of different non - adherent tendon solutions to reduce short - term deflection in full - scale timber - concrete - composite T - section beams, J. Build. Eng., 31, pp. 101437, DOI: 10.1016/j.jobe.2020.101437.

[3] Dias, A., Schänzlin, J., Dietsch, P. (2018). Design of timber-concrete composite structures.

[4] Tao, H., Yang, H., Zhang, J., Ju, G., Xu, J., Shi, B. (2022). Nonlinear finite element analysis on timber-concrete composite beams, J. Build. Eng., 51, pp. 104259, DOI: 10.1016/j.jobe.2022.104259.

[5] Lamothe, S., Sorelli, L., Blanchet, P., Galimard, P. (2020). Engineering ductile notch connections for composite floors made of laminated timber and high or ultra-high performance fiber reinforced concrete, Eng. Struct., 211, pp. 110415, DOI: 10.1016/j.engstruct.2020.110415.

[6] Bao, Y., Lu, W., Yue, K., Zhou, H., Lu, B., Chen, Z. (2022). Structural performance of cross-laminated timber-concrete composite floors with inclined self-tapping screws bearing unidirectional tension-shear loads, J. Build. Eng., 55, pp. 104653, DOI: 10.1016/j.jobe.2022.104653.

[7] Zhang, L., Zhou, J., Chui, Y.H. (2022). Development of high-performance timber-concrete composite floors with reinforced notched connections, Structures, 39(December 2021), pp. 945–957, DOI: 10.1016/j.istruc.2022.03.074.

[8] Deresa, S., Xu, J., Demartino, C., Minafò, G., Camarda, G. (2021). Static Performances of Timber-and Bamboo-Concrete Composite Beams: A Critical Review of Experimental Results, Open Constr. Build. Technol. J., 15, pp. 17–54, DOI: 10.2174/1874836802115010017.

[9] Jiang, Y., Crocetti, R. (2019). CLT-concrete composite floors with notched shear connectors, Constr. Build. Mater., 195, pp. 127–139, DOI: 10.1016/j.conbuildmat.2018.11.066.

[10] Denouwe, D., Messan, A., Fournely, E., Bouchaïr, A. (2018). Experimental study of the mechanical behavior of timber-concrete shear connections with threaded reinforcing bars, Eng. Struct., 172, pp. 997–1010, DOI: 10.1016/j.engstruct.2018.06.084.

[11] Yeoh, D. (2010).Behaviour and Design of Timber-Concrete Composite Floor Sytem. University of Canterbury. Department of Civil and Natural Resources.

[12] Ling, Z., Zhang, H., Mu, Q., Xiang, Z., Zhang, L., Zheng, W. (2022). Shear performance of assembled shear connectors for timber–concrete composite beams, Constr. Build. Mater., 329, pp. 127158, DOI: 10.1016/j.conbuildmat.2022.127158.

[13] Zhang, L., Chui, Y.H., Tomlinson, D. (2020). Experimental investigation on the shear properties of notched connections in mass timber panel-concrete composite floors, Constr. Build. Mater., 234, pp. 117375, DOI: 10.1016/j.conbuildmat.2019.117375.

[14] Yeoh, D., Fragiacomo, M., Deam, B. (2011). Experimental behaviour of LVL–concrete composite floor beams at

strength limit state, Eng. Struct., 33(9), pp. 2697–2707, DOI: 10.1016/j.engstruct.2011.05.021.
[15] Madqour, M., Hassan, H., Fawzy, K. (2021). Finite element modeling of flexural behavior of reinforced concrete beams externally strengthened with CFRP sheets, Frat. Ed Integrita Strutt., 15(59), pp. 62–77, DOI: 10.3221/IGF-ESIS.59.05.
[16] Boursas, F., Boutagouga, D. (2021). Parametric study of I-shaped shear connectors with different orientations in push-out test, Frat. Ed Integrita Strutt., 15(57), pp. 24–39, DOI: 10.3221/IGF-ESIS.57.03.
[17] Dias, A.M.P.G., Jorge, L.F.C. (2011). The effect of ductile connectors on the behaviour of timber-concrete composite beams, Eng. Struct., 33(11), pp. 3033–3042, DOI: 10.1016/j.engstruct.2011.05.014.
[18] Yeoh, D. (2010). Behaviour and Design of Timber-Concrete Composite Floor Sytem, pp. 189.
[19] Chen, G., He, B. (2017). Stress-strain Constitutive Relation of OSB under Axial Loading: An Experimental Investigation, 12(2000), pp. 6142–6156.
[20] Oudjene, M., Meghlat, E.M., Ait-Aider, H., Lardeur, P., Khelifa, M., Batoz, J.-L. (2018). Finite element modelling of the nonlinear load-slip behaviour of full-scale timber-to-concrete composite T-shaped beams, Compos. Struct., 196, pp. 117–126, DOI: 10.1016/j.compstruct.2018.04.079.
[21] Estévez-Cimadevila, J., Martín-Gutiérrez, E., ruárez-Riestra, F., Otero-Chans, D., Vázquez-Rodríguez, J.A. (2022). Timber-concrete composite structural flooring system, J. Build. Eng., pp. 104078, DOI: 10.1016/j.jobe.2022.104078.